Reports

Magmatic Resurgence in Long Valley Caldera, California: Possible Cause of the 1980 Mammoth Lakes Earthquakes

Abstract. *Changes in elevation between 1975 and October 1980 along a leveling line across the Long Valley caldera indicate a broad (half-width, 15 kilometers) uplift (maximum, 0.25 meter) centered on the old resurgent dome. This uplift is consistent with reinflation of a magma reservoir at a depth of about 10 kilometers. Stresses generated by this magmatic resurgence may have caused the sequence of four magnitude 6 earthquakes near Mammoth Lakes in May 1980.*

The Long Valley caldera (Fig. 1), an elliptical depression about 30 km long by 15 km wide, was formed 0.7 million years ago by collapse of the magma chamber after an explosive eruption that ejected approximately 600 km^3 of rhyolitic magma. Within 0.1 million years after the collapse, replenishment of magma within the reservoir caused a swelling (resurgent dome) in the west half of the caldera that presumably marks the center of the buried reservoir (*1*). Current research indicates that there were at least ten eruptions in the western caldera and Mono Craters during the last 1500 years, including several explosive eruptions and extrusion of rhyolite domes during the last 400 years (*2*).

An unusual sequence of earthquakes began just south of the Long Valley caldera on 4 October 1978 with a magnitude 5.7 earthquake (epicenter coincides with position of station S in Fig. 1) and culminated with four magnitude 6 earthquakes (Fig. 1) on 25 and 27 May 1980. Subsequent activity has included a magnitude 5.7 earthquake on 30 September 1981 (epicenter about 2 km southeast of station L in Fig. 1). The long duration (1978 to 1981), unusual migration pattern, and swarmlike behavior of this earthquake sequence (*3*) are not typical of tectonic earthquakes in California.

In connection with studies of the Mammoth Lakes earthquake sequence, a 36-km-long section of a first-order leveling line (Fig. 1) surveyed in 1932, 1957, and 1975 was resurveyed in October 1980. The 1980 elevations were calculated relative to the bench mark at the southeast end of the line, and the elevation of that bench mark was arbitrarily taken to be the same as its 1975 elevation. Figure 2B shows the elevation change in 1980 relative to 1975 for each bench mark as a function of the distance along the leveling line from its northwest end. The maximum measured uplift (0.25 m) is ten times more than could reasonably be attributed to surveying errors over such a short distance and small elevation difference (*4*).

Although we initially assumed that the observed elevation changes were an effect of the Mammoth Lakes earthquakes, it became apparent that these changes are more closely correlated with the known structure of the Long Valley caldera. In particular, the elevation changes seem to represent a symmetrical uplift centered on the resurgent dome in the west half of the caldera. Similar uplifts observed near Socorro, New Mexico (*5*), and Yellowstone National Park, Wyoming (*6*), have been attributed to the influx of magma into midcrustal reservoirs. Therefore, we compared (Fig. 2) the observed elevation changes with the predicted uplift associated with inflation of a spherical magma chamber centered beneath the resurgent dome, a model commonly used to explain the swelling observed at active volcanoes (*7*). The disposable parameters in the model are the depth to the center of the magma chamber and the volume of magma injected into the chamber, taken here to be 11 km and 0.15 km^3, respectively; the radius of the chamber is not critical. In comparing the profiles of observed elevation changes and predicted uplift in Fig. 2, the profile of observed changes should be translated vertically upward so that it coincides with that of predicted uplift on the right-hand side of the graph. (The elevation change there was arbitrarily set at zero in constructing the profile of observed elevation changes.) The agreement between the two profiles is good; the only significant discrepancy occurs at the crossing of the Hilton Creek fault, where the deviations (up on the left and down on the right) are explainable by the observed normal slip that occurred on that fault on 25 May 1980 (*8*).

Horizontal deformation in the Mammoth Lakes area was determined from precise trilateration surveys in 1972, 1973, 1976, 1979, and 1980 (*9*). The solid arrows in Fig. 1 show the displacements of the trilateration stations between July 1979 and September 1980, as inferred from the last two surveys. The error bars at the end of each vector define the principal axes of the ellipse representing 95 percent confidence. In deducing these displacements, we assumed that station T is fixed and the azimuth from station T to station CH did not change. Attempts to explain this displacement pattern by slip on the Hilton Creek fault or other faults in the epicentral area of the Mammoth Lakes earthquakes have been unsuccessful (*9*).

The dashed arrows in Fig. 1 show the

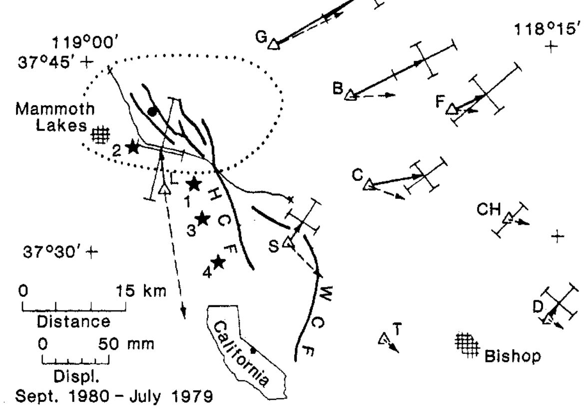

Fig. 1. Northern Owens Valley, California, showing locations of Long Valley caldera (dotted ellipse), leveling line (sinuous line connecting **x**'s), trilateration stations (triangles), Hilton Creek fault (*HCF*), Wheeler Crest fault (*WCF*), epicenters of magnitude 6 earthquakes (stars, numbered in order of occurrence), center of resurgent dome within caldera (●), and towns of Mammoth Lakes and Bishop. Solid arrows at trilateration stations represent displacement observed over the interval July 1979 to September 1980; dashed arrows represent displacements expected from expansion of a buried magma chamber.

0036-8075/82/0806-0531$01.00/0

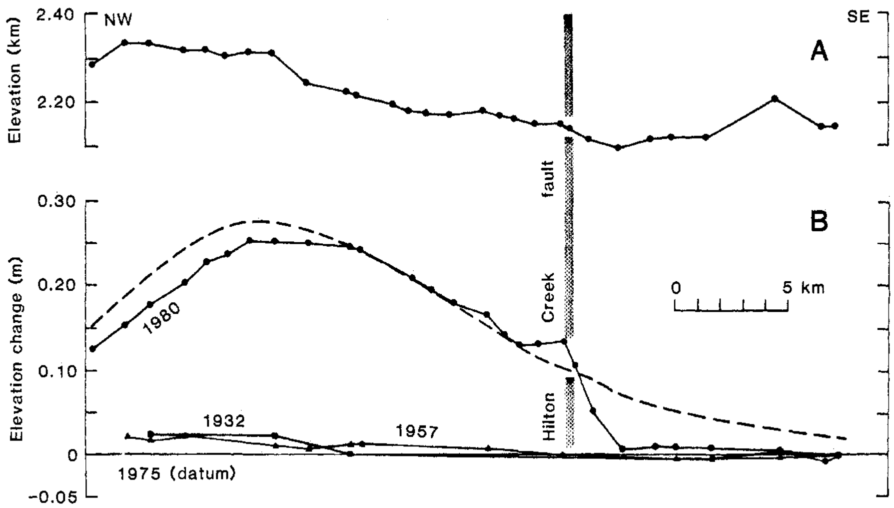

Fig. 2. (A) Elevation and (B) elevation change of bench marks as a function of distance from northwest to southeast along leveling line shown in Fig. 1. Solid curves in (B) are the 1980, 1957, and 1932 elevations less the 1975 elevations; dashed curve is the elevation change expected from expansion of a buried magma chamber.

displacements predicted for the trilateration stations from the same model used to predict the uplift in Fig. 2. Because station T was arbitrarily held fixed in calculating the observed displacements in Fig. 1, a proper comparison with the predicted displacements requires that the displacement predicted at station T (14 mm to the southeast) be added to each of the observed displacements. Then the predicted displacements agree reasonably well in direction and agree within a factor of about 2 in magnitude with the observed displacements except at stations S and L, where the displacement discrepancies (observed minus predicted displacement) amount to 30 and 120 mm, respectively, northward at both stations. We infer that these discrepancies represent coseismic displacement generated by the Mammoth Lakes earthquake sequence because both stations lie within the epicentral area. However, the nodal-plane solutions for the main earthquakes in the Mammoth Lakes sequence suggest left-lateral slip on near-vertical north-striking fault planes (*10*). Northward displacement at both station S and station L would then require that the principal rupture be west of station L, whereas the north-south alignment of three of the four magnitude 6 shocks would suggest that the rupture was east of station L. However, the overall distribution of foreshocks, main shocks, and aftershocks leaves some doubt whether a single rupture plane was involved.

Because the elevations determined in 1932 and 1957 by surveys of the leveling line shown in Fig. 1 do not differ significantly from the 1975 elevations (Fig. 2), magma injection could not have begun before summer 1975. Comparison of the 1972, 1973, 1976, 1979, and 1980 trilateration surveys shows that significant changes occurred only in the interval from July 1979 to September 1980 (*9*). Thus it is unlikely that any substantial expansion of the magma chamber occurred before July 1979. The Mammoth Lakes earthquake sequence began somewhat earlier with a magnitude 5.7 event located approximately beneath station S (Fig. 1) on 4 October 1978. However, most of the swarm activity and all four of the magnitude 6 events occurred after the July 1979 trilateration survey (*10*).

Several lines of evidence suggest that the observed large-scale deformation was more likely caused by magmatic inflation of a midcrustal reservoir than by coseismic deformation associated with the Mammoth Lakes earthquake sequence: (i) the good fit between the observed uplift and that predicted by the magma chamber inflation model (Fig. 2); (ii) our inability to model the observed deformation adequately by faulting in the epicentral area, particularly if this faulting was only strike-slip, as suggested by the nodal-plane solutions; and (iii) the long duration (1978 to 1981), unusual migration patterns, and swarmlike seismicity, not typical of tectonic events in California.

If the large-scale deformation is a consequence of magma injection, then it may be that the Mammoth Lakes earthquakes were caused (or at least triggered) by the stresses associated with magma injection. As a partial test of this explanation, we used the magma chamber expansion model to calculate the stress field at the hypocenters of the magnitude 6 earthquakes and then determined whether that field was consistent with the observed nodal-plane solutions. The stress field is best described in cylindrical coordinates, with the z-axis vertical and passing through the center of the magma chamber; the nonzero stress components are σ_{rr}, $\sigma_{\theta\theta}$, σ_{zz}, and σ_{zr}. At the 5- to 13-km depths at which earthquakes occur, σ_{rr} is negative (compressive), $\sigma_{\theta\theta}$ and σ_{zz} are positive (tensile) and about equal, and σ_{zr} is relatively small. The nodal-plane solutions (*10*) for the magnitude 6 earthquakes are consistent with left-lateral slip on near-vertical planes that strike approximately north-south. We find the horizontal shear stress (left-lateral shear positive) on these planes to be as follows (earthquakes numbered in Fig. 1): earthquake 1, 1 MPa; earthquake 2, −1 MPa; earthquake 3, 0.2 MPa; and earthquake 4, 0.1 MPa. Left-lateral shear on the north-striking nodal plane would also be imposed at the hypocenters of the 4 October 1978 earthquake (0.05 MPa) and the 30 September 1981 earthquake (0.4 MPa). The dip-slip component of shear is in all cases much smaller than the horizontal component. The normal stress imposed across each fault plane is tensile. Thus the stresses imposed by expansion of the magma chamber are consistent with the observed focal mechanisms for all the earthquakes except 2, for which the nodal-plane solution is notably weak.

The stress field generated by expansion of a buried magma chamber is also consistent with the surface rupture observed after the May 1980 earthquakes. Normal slip occurred along the northern part of the Hilton Creek fault both southeast of the caldera and along a broad zone of splayed extensional faults striking northwest within the caldera and extending to the center of the resurgent dome (*8*). Within this broad zone of fractures, both nonzero components of stress (σ_{rr} and $\sigma_{\theta\theta}$) are tensile and $\sigma_{\theta\theta} > \sigma_{rr}$. Along the Hilton Creek fault outside the caldera, $\sigma_{\theta\theta}$ is tensile and σ_{rr} compressive; the component of stress perpendicular to the fault trace is about 0.3 MPa tension.

J. C. Savage
M. M. Clark
U.S. Geological Survey, Menlo Park, California 94025

References and Notes

1. R. A. Bailey, G. B. Dalrymple, M. A. Lanphere, *J. Geophys. Res.* **81**, 725 (1976); R. T. Kilbourne, C. W. Chesterman, S. H. Wood, *Calif. Div. Mines Geol. Spec. Rep. 150* (1980), p. 7.
2. C. D. Miller and R. A. Bailey, personal communication.
3. A. Ryall and F. Ryall, *Calif. Div. Mines Geol. Spec. Rep. 150* (1980), p. 27; F. Ryall and A. Ryall, *Geophys. Res. Lett.* **8**, 557 (1981).
4. G. Bomford, *Geodesy* (Oxford Univ. Press, London, ed. 3, 1971), pp. 239–246.

5. R. Reilinger and J. Oliver, *Geology* **4**, 583 (1976); ______, L. Brown, A. Sanford, E. Balazs, *ibid.* **8**, 291 (1980).
6. J. R. Pelton and R. B. Smith, *Science* **206**, 1179 (1979).
7. K. Mogi, *Bull. Earthquake Res. Inst. Tokyo* **36**, 99 (1958); R. S. Fiske and W. T. Kinoshita, *Science* **165**, 341 (1969); J. H. Dieterich and R. W. Decker, *J. Geophys. Res.* **80**, 4094 (1975).
8. G. C. Taylor and W. A. Bryant, *Calif. Div. Mines Geol. Spec. Rep. 150* (1980), p. 49; M. M. Clark, J. C. Yount, P. R. Vaughan, R. L. Zepeda, *U.S. Geol. Surv. Misc. Field Invest. Map MF 1396*, in press.
9. J. C. Savage, M. Lisowski, W. H. Prescott, N. E. King, *Bull. Seismol. Soc. Am.* **71**, 465 (1981).
10. C. H. Cramer and T. R. Toppozada, *Calif. Div. Mines Geol. Spec. Rep. 150* (1980), p. 91.
11. We appreciate the cooperation of California Department of Transportation in the 1980 leveling and the assistance of R. O. Castle in the analysis of the 1932 and 1957 leveling data.

16 November 1981; revised 18 February 1982

Ancient Maya Mercury

Abstract. *Discovery of mercury in an ancient Maya offering at Lamanai, Belize, has stimulated examination of possible sources of the material in the Maya area. Two zones of cinnabar and native mercury deposits can be defined in the Maya highlands, and the presence of the native metal suggests that the ancient Maya collected rather than extracted the mercury from ore.*

Excavation of the ancient Maya site of Lamanai in northern Belize (Fig. 1) has revealed extensive evidence of a rich Postclassic and early historic occupation (A.D. 900 to 1675), as well as remains from an earlier period (600 B.C. to A.D. 900) (*1*). In 1980, offerings associated with stelae and other monuments were recovered; among these was the giant marker disc at the center of the lone ballcourt at the site. Raising of the disc, (1.5 m in diameter) revealed an offering in a lidded bowl; the vessel contained more than 100 g of crystalline hematite, mostly in powder form, and artifacts that included two miniature vessels, in one of which was approximately 19 g of cinnabar (HgS). The vessels and a number of objects of jade, shell, and pearl sat atop a pool of 9.7 cm^3 (131.9 g) of mercury (Fig. 2). Slip and shape characteristics of the container vessel and two fragmented dishes on which it rested fix the date of the offering and the ballcourt construction in the late 9th or early 10th century A.D.

The ballcourt offering is evidence of ceremonial activity at the central Maya lowland site of Lamanai at the end of the Classic period. Previously, mercury was known only from highland sites about 275 km to the south: Copán and nearby El Paraiso in Honduras (*2*); Quiriguá in Guatemala, some 45 km north of Copán (*3*); and Kaminaljuyú (*4*) and neighboring Lake Amatitlán (*5*), approximately 140 km west of Copán (Fig. 1). Thus the Lamanai discovery extends both the known geographic distribution and the time span of mercury use by the Maya. These aspects of the discovery prompted a review of data on possible sources of the metal.

Mercury usually occurs as cinnabar, and cinnabar was prized by the Maya as pigment, apparently because its color was symbolic of blood and blood sacrifice; it was included in offerings and elite burials, not infrequently in association with crystalline hematite (*6, 7*). It has been assumed that the cinnabar found in lowland sites in Guatemala, Belize, and the Yucatán Peninsula came from the Maya highlands and was important in highland-lowland Maya trade (*6*). Most of the Yucatán Peninsula is mineralogically impoverished, but the Sierra Madre mountains of southern Mexico, Guatemala, and Honduras are geologically suitable for the occurrence of HgS deposits.

Without trace-element analyses of HgS from a wide range of highland and lowland sites, it is not possible to identify specific sources with any degree of certainty. Fuson (*8*) proposed a source in the Mexican state of Chiapas for cinnabar traded to the Maya lowlands, but there is neither archeological nor direct geological support for the suggestion. There are, however, HgS deposits in the Early Cretaceous Todos Santos Formation of Guatemala near Nahualá, Department of Sololá, and Zunil, Department of Quetzaltenango (*9*), both west-northwest of Lake Atitlán. Native mercury appears to have been collected in Quetzaltenango (*10*) and in the area of San Miguel Acatán, Department of Huehuetenango (*11*) (Fig. 1). A second zone of HgS occurs in

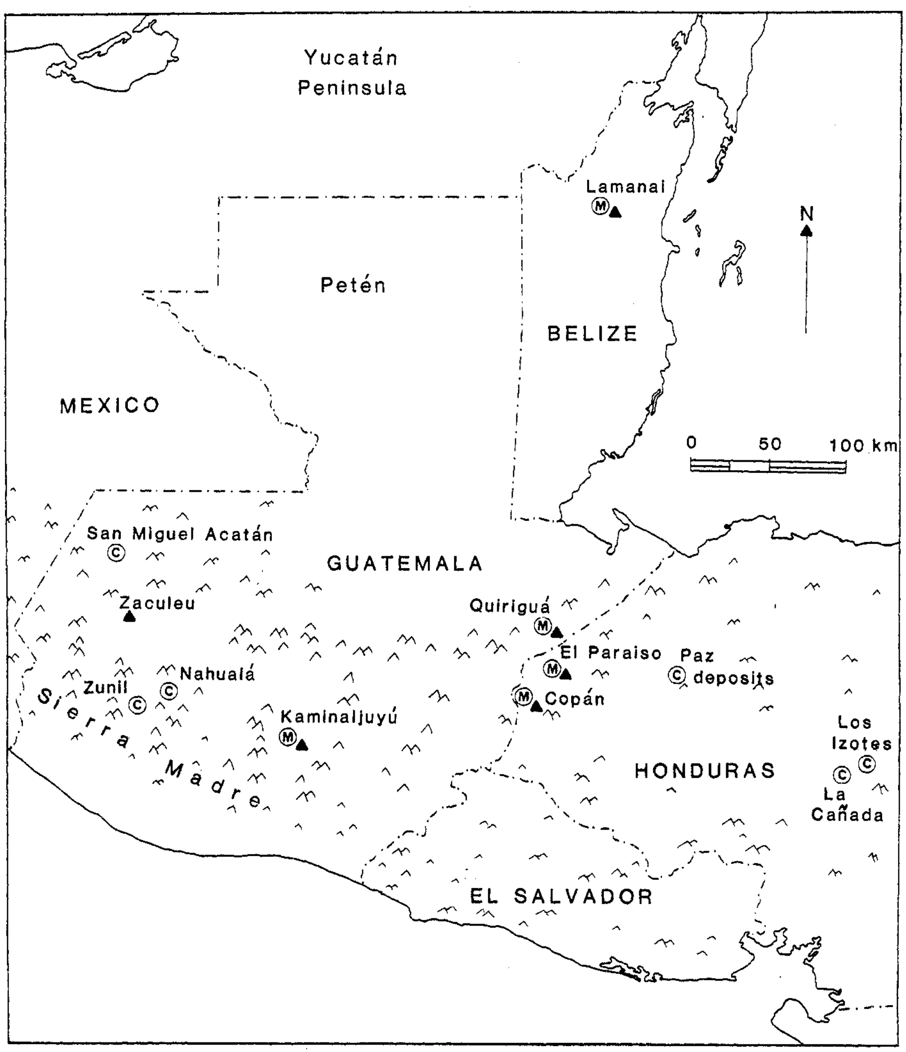

Fig. 1. Map of Maya Area. *C*, HgS and native mercury sources; ▲, archeological sites; and *M*, archeological sites yielding mercury.